

# A Comparison of the Ability of Leu<sup>8</sup>- and Pro<sup>8</sup>-Oxytocin to Regulate Intracellular Ca<sup>2+</sup> and Ca<sup>2+</sup>-Activated K<sup>+</sup> Channels at Human and Marmoset Oxytocin Receptors<sup>§</sup>

Marsha L. Pierce, Suneet Mehrotra, Aaryn C. Mustoe, Jeffrey A. French, and Thomas F. Murray

Department of Pharmacology, Creighton University School of Medicine, Omaha, Nebraska (M.L.P., S.M., T.F.M.); and Department of Psychology, University of Nebraska, Omaha, Nebraska (A.C.M., J.A.F.)

Received September 26, 2018; accepted January 30, 2019

## ABSTRACT

The neurohypophyseal hormone oxytocin (OT) regulates biologic functions in both peripheral tissues and the central nervous system. In the central nervous system, OT influences social processes, including peer relationships, maternal-infant bonding, and affiliative social relationships. In mammals, the nonapeptide OT structure is highly conserved with leucine in the eighth position (Leu<sup>8</sup>-OT). In marmosets (*Callithrix*), a nonsynonymous nucleotide substitution in the *OXT* gene codes for proline in the eighth residue position (Pro<sup>8</sup>-OT). OT binds to its cognate G protein-coupled receptor (OTR) and exerts diverse effects, including stimulation (G<sub>s</sub>) or inhibition (G<sub>i/o</sub>) of adenylyl cyclase, stimulation of potassium channel currents (G<sub>i</sub>), and activation of phospholipase C (G<sub>q</sub>). Chinese hamster ovary cells expressing marmoset or human oxytocin receptors (mOTRs or hOTRs, respectively) were used to characterize OT signaling. At the mOTR, Pro<sup>8</sup>-OT was more efficacious than Leu<sup>8</sup>-OT in measures

of G<sub>q</sub> activation, with both peptides displaying subnanomolar potencies. At the hOTR, neither the potency nor efficacy of Pro<sup>8</sup>-OT and Leu<sup>8</sup>-OT differed with respect to G<sub>q</sub> signaling. In both mOTR- and hOTR-expressing cells, Leu<sup>8</sup>-OT was more potent and modestly more efficacious than Pro<sup>8</sup>-OT in inducing hyperpolarization. In mOTR cells, Leu<sup>8</sup>-OT-induced hyperpolarization was modestly inhibited by pretreatment with pertussis toxin (PTX), consistent with a minor role for G<sub>i/o</sub> activation; however, the Pro<sup>8</sup>-OT response in mOTR and hOTR cells was PTX insensitive. These findings are consistent with membrane hyperpolarization being largely mediated by a G<sub>q</sub> signaling mechanism leading to Ca<sup>2+</sup>-dependent activation of K<sup>+</sup> channels. Evaluation of the influence of apamin, charybdotoxin, paxilline, and TRAM-34 demonstrated involvement of both intermediate and large conductance Ca<sup>2+</sup>-activated K<sup>+</sup> channels.

## Introduction

Oxytocin (OT) is a nonapeptide that regulates a host of physiologic functions both peripherally (e.g., uterine contraction, lactation) and centrally (e.g., social behavior). OT is synthesized in the magnocellular neurons of the supraoptic and paraventricular nuclei of the hypothalamus, and OT

neurons primarily project to the posterior pituitary where OT is released into the bloodstream (Ludwig and Leng, 2006). OT neurons also project to multiple regions within the “social brain” (Stoop, 2014). These latter OT projections are thought to be responsible for the modulation of many behaviors, including social recognition and memory, sexual behavior, parental care, pair-bond formation and maintenance, and cooperation and aggression (Insel et al., 2010; Johnson and Young, 2015). Dysfunction in OT signaling has also been widely reported in mental health outcomes in which social deficits are commonly observed, such as schizophrenia and depression/anxiety. Consequently, OT has received considerable interest as a therapeutic for these disorders but studies have shown mixed results (Young and Barrett, 2015; Guastella and Hickie, 2016; Parker et al., 2017).

This work was supported by the National Institutes of Health Eunice Kennedy Shriver National Institute of Child Health and Human Development [Grant R01-HD089147].

This work was previously presented as a poster presentation at the following meeting: Pierce ML, Mehrotra S, Toews ML, French JA, and Murray TF (2016) Comparison of Leu<sup>8</sup>- and Pro<sup>8</sup>-oxytocin potency, efficacy and functional selectivity at the human and marmoset receptors. *Neuroscience* 2016; 2016 Nov 12-16; San Diego, CA.

<https://doi.org/10.1124/mol.118.114744>.

<sup>§</sup> This article has supplemental material available at molpharm.aspetjournals.org.

**ABBREVIATIONS:** BAPTA-AM, 1,2-bis(2-aminophenoxy)ethane-*N,N,N',N'*-tetraacetic acid tetrakis(acetoxymethyl ester); BK<sub>Ca</sub>, large conductance Ca<sup>2+</sup>-activated potassium channel; CHO, Chinese hamster ovary; CI, confidence interval; DMSO, dimethylsulfoxide; E<sub>max</sub>, maximum response achievable; FBS, fetal bovine serum; FLIPR, fluorescence imaging plate reader; FMP, fluorescence imaging plate reader membrane potential; GIRK, G protein-coupled inwardly rectifying potassium channel; GPCR, G protein-coupled receptor; HEK, human embryonic kidney; hOTR, human oxytocin receptor; IK<sub>Ca</sub>, intermediate conductance Ca<sup>2+</sup>-activated potassium channel;  $\kappa$ OR,  $\kappa$ -opioid receptor; Leu<sup>8</sup>-OT, consensus mammalian oxytocin sequence; mOTR, marmoset oxytocin receptor; NWM, New World monkey; OT, oxytocin; OTR, oxytocin receptor; PLC, phospholipase C; Pro<sup>8</sup>-OT, oxytocin sequence with proline in the eighth position; PTX, pertussis toxin; SERCA, sarco/endoplasmic reticulum Ca<sup>2+</sup> ATPase; SK<sub>Ca</sub>, small conductance Ca<sup>2+</sup>-activated potassium channel.

OT-like nonapeptides are highly conserved signaling molecules that activate G protein-coupled receptors (GPCRs). OT binds primarily to the oxytocin receptor (OTR) and, to a lesser extent, the related nonapeptide vasopressin receptors (Gimpl and Fahrenholz, 2001; Manning et al., 2008). The OTR promiscuously couples to and activates multiple G proteins producing diverse effects on cellular function, including inhibition of adenylyl cyclase ( $G_{i/o}$ ), stimulation of potassium channel currents ( $G_i$ ), and activation of phospholipase C ( $G_q$ ) (Reversi et al., 2005). OTR activation also leads to a variety of signaling responses, which suggests that OT activation may preferentially bias specific G-protein pathways that vary across cell types both within the brain and in the periphery. For example,  $G_q$  activation mediates activation of neural OTRs that generate pulsatile OT secretion (Wang and Hatton, 2007), whereas both  $G_{i/o}$  and  $G_q$  activation mediate  $Ca^{2+}$  mobilization and GTP hydrolysis in myometrial cells (Phaneuf et al., 1993).

Despite the high degree of conservation of the OT ligand among most mammals, many New World monkeys (NWMs) possess OT sequence modifications that have evolved from the ancestral mammalian OT sequence (Cys-Tyr-Ile-Gln-Asn-Cys-Pro-Leu-Gly; Leu<sup>8</sup>-OT). Thus far, five additional OT-like variants have been identified with variability in amino acids mainly at position 8, but also at positions 2 and 3 (Lee et al., 2011; Wallis, 2012; Ren et al., 2015; Vargas-Pinilla et al., 2015). The most common OT variant is a Leu-to-Pro substitution at the eighth amino acid position (Pro<sup>8</sup>-OT). This substitution significantly alters the linear portion of the ligand's three-dimensional architecture, whereby formation of the Pro-Pro polyproline helix in the linear portion of the OT ligand could potentially lead to changes in OT interaction with the OTR with attendant alteration in potency and/or efficacy (Zingg and Laporte, 2003; Geisler and Chmielewski, 2009).

Differences between OT and the related nonapeptide vasopressin (which differs in amino acid positions 3 and 8) show select ligand recognition with specific portions of the OTR and vasopressin receptor 1A, potentially suggesting important OTR recognition features that could change as a function of a Leu-to-Pro substitution in position 8 (Chini et al., 1995, 1996; Zingg and Laporte, 2003). OT ligand variants are also of interest because these ligands show significant coevolution with corresponding OTR sequence structures as well as a significant association with the presence of social phenotypes, including social monogamy and paternal care in primates (Ren et al., 2015; Vargas-Pinilla et al., 2015), and these social phenotypes are known to be influenced by exogenous OT treatments (French et al., 2016). The association between OT/OTR structures with social behavior in NWMs raises the possibility that OT-related phenotypic differences might be a consequence of functional selectivity with respect to the signaling properties associated with OT analog (e.g., Pro<sup>8</sup>-OT) activation of OTRs. Currently, there is limited information regarding signaling profiles of OT analogs at human and marmoset oxytocin receptors (hOTRs and mOTRs, respectively).

To assess whether OT/OTR variability results in altered pharmacological properties of OT ligands, we stably transfected Chinese hamster ovary (CHO) cells expressing hOTRs or mOTRs and examined the resulting activation of OT-OTR signaling pathways. We evaluated whether OT ligand variation resulted in distinct activation of different G protein-mediated

cell-signaling pathways ( $G_{i/o}$  and  $G_q$ ) in hOTR- and mOTR-expressing cells, as assessed by elevation of intracellular  $Ca^{2+}$  or alteration in membrane potential.

## Materials and Methods

**CHO Cell Cultures.** Wild-type CHO-K1 cells were purchased from American Type Culture Collection (CCL-61) and cultured in Ham's F-12 medium (SH30026.01; Hyclone), 10% fetal bovine serum (FBS) (S11550; Atlanta Biologicals), 1.5% HEPES 1 M solution (SH30231.01; Hyclone), and 1% penicillin-streptomycin (10,000 U/ml, 15140-163; Life Technologies). hOTR-expressing CHO-K1 cell lines were purchased from Genscript (M00195). mOTR plasmid was purchased from Genscript and stably transfected into CHO-K1 cells. hOTR- and mOTR-expressing cells were cultured in Ham's F-12 medium (SH30026.01; Hyclone), 10% FBS (S11550; Atlanta Biologicals), 1.5% HEPES 1 M solution (SH30231.01; Hyclone), 1% penicillin-streptomycin (10,000 U/ml, 15140-163; Life Technologies), and 400 mg/ml G418 (G64000-5.0; RPI Corp.).  $\kappa$ -Opioid receptor ( $\kappa$ OR)-expressing CHO ( $\kappa$ OR-CHO) cells were cultured in RPMI 1640 medium supplemented with 10% FBS (S11550; Atlanta Biologicals). Cells were cultured at 37°C in 5% CO<sub>2</sub> and 90% humidity.

**CHO Cell Stable Transfection and Selection of Clones.** CHO-K1 cells ( $1 \times 10^6$ ) were electroporated with 1.5  $\mu$ g vector encoding mOTR plasmid (Genscript). After transfection, cells were seeded on 10-cm plates and grown under antibiotic pressure with 400 mg/ml G418 (G64000-5.0; RPI Corp.) for 72 hours. The clones were picked using cloning cylinders (3166-10; Corning), and 50  $\mu$ l 0.05% trypsin (25300-054; GIBCO) was added to the cells/colony and detached by pipetting two to three times. Dissociated cells were diluted in 100 ml media and plated in 24-well plates (~1 cell/well). The cells were allowed to grow under antibiotic pressure for 3 weeks, with media change every 72 hours. Five clones were picked for a fluorescence imaging plate reader (FLIPR) membrane potential (FMP) assay. Among all five clones, clone 2 showed maximum responses to Leu<sup>8</sup>-OT and Pro<sup>8</sup>-OT in decreasing the FMP blue fluorescence and was selected for further studies.

**Drugs.** Leu<sup>8</sup>-OT (66-0-52; American Peptide Company) and Pro<sup>8</sup>-OT (58863; Anaspec) were reconstituted in dimethylsulfoxide (DMSO) (D4540; Sigma-Aldrich). Charybdotoxin (C7802; Sigma-Aldrich) was reconstituted in ultrapure water. 1,2-Bis(2-aminophenoxy)ethane-*N,N,N',N'*-tetraacetic acid tetrakis(acetoxymethyl ester) (BAPTA-AM) (A1076; Sigma-Aldrich), M119K (1198893; Developmental Therapeutics Program, National Cancer Institute), NS-1619 (N170; Sigma-Aldrich), paxilline (P2928; Sigma-Aldrich), SKA-31 (S5573; Sigma-Aldrich), thapsigargin (T9033; Sigma-Aldrich), and TRAM-34 (T6700; Sigma-Aldrich) were reconstituted in DMSO. Pertussis toxin (PTX) (P7208; Sigma-Aldrich) was reconstituted in ultrapure water with 5 mg/ml bovine serum albumin (BP1600-100; Fisher Scientific). Dynorphin A (1-13) amide (26-4-51A; American Peptide Company) was dissolved in 25 mM Tris at pH 7.4. Apamin (A1289; Sigma-Aldrich) was reconstituted in 0.05 M acetic acid.

**Intracellular Calcium Mobilization Assay.** The effect of OT addition on intracellular calcium mobilization was examined using Fluo3-AM fluorescence (F1241; Molecular Probes) monitored with a FLIPR2 plate reader (Molecular Devices). FLIPR operates by illuminating the bottom of a 96-well microplate with an air-cooled laser and measuring the fluorescence emissions from cell-permeant dyes in all 96 wells simultaneously using a cooled charge-coupled device camera. This instrument is equipped with an automated 96-well pipettor, which can be programmed to deliver precise quantities of solutions simultaneously to all 96 culture wells from two separate 96-well source plates.

Cells were plated at 0.3 million cells/ml in 96-well plates (P9803; MidSci) and cultured overnight in culture media at 37°C in 5% CO<sub>2</sub> and 95% humidity. On the day of assay, growth medium was aspirated and replaced with 100  $\mu$ l dye-loading medium per well containing

4  $\mu\text{M}$  Fluo-3 AM and 0.04% pluronic acid (P3000MP; Molecular Probes) in Locke's buffer (8.6 mM HEPES, 5.6 mM KCl, 154 mM NaCl, 5.6 mM glucose, 1.0 mM  $\text{MgCl}_2$ , and 2.3 mM  $\text{CaCl}_2$ , pH 7.4). Cells were incubated for 1 hour at 37°C in 5%  $\text{CO}_2$  and 95% humidity and then washed four times in 180  $\mu\text{l}$  fresh Locke's buffer using an automated microplate washer (Bio-Tek Instruments Inc.). Baseline fluorescence was recorded for 60 seconds, prior to a 20  $\mu\text{l}$  addition of various concentrations of Leu<sup>8</sup>-OT and Pro<sup>8</sup>-OT. Cells were excited at 488 nm and  $\text{Ca}^{2+}$ -bound Fluo-3 emission was recorded at 538 nm at 2-second intervals for an additional 200 seconds.

To assess the role of intracellular calcium in the OT mobilization of calcium, the sarco/endoplasmic reticulum  $\text{Ca}^{2+}$  ATPase (SERCA) inhibitor thapsigargin was used to rapidly deplete intracellular calcium stores. Thapsigargin inhibition of calcium mobilization in prostate cancer cells is complete in less than 5 minutes (Sehgal et al., 2017). Cells were incubated in 100  $\mu\text{l}$  dye-loading medium per well containing 4  $\mu\text{M}$  Fluo-3 AM and 0.04% pluronic acid in Locke's buffer (8.6 mM HEPES, 5.6 mM KCl, 154 mM NaCl, 5.6 mM glucose, 1.0 mM  $\text{MgCl}_2$ , 2.3 mM  $\text{CaCl}_2$ , and 0.5 mM probenecid, pH 7.4), at 37°C in 5%  $\text{CO}_2$  and 95% humidity for 60 minutes prior to washing four times in 180  $\mu\text{l}$  Locke's buffer and 10  $\mu\text{l}$  addition of thapsigargin (1  $\mu\text{M}$  final concentration) and incubated for an additional 5 minutes. Intracellular calcium mobilization assays were performed as described above.

**Membrane Potential Assay.** The FLIPR Membrane Potential Assay (FMP blue, F1241; Molecular Probes) was used to assess changes in membrane potential. Confluent cells were plated at 0.3 million cells/ml in 96-well plates (P9803; MidSci) and cultured overnight in culture media at 37°C in 5%  $\text{CO}_2$  and 95% humidity. The growth medium was removed and replaced with 190  $\mu\text{l}$  per well of FMP blue in Locke's buffer (8.6 mM HEPES, 5.6 mM KCl, 154 mM NaCl, 5.6 mM glucose, 1.0 mM  $\text{MgCl}_2$ , and 2.3 mM  $\text{CaCl}_2$ , pH 7.4). Cells were incubated at 37°C in 5%  $\text{CO}_2$  and 95% humidity for 45 minutes. Baseline fluorescence was recorded for 60 seconds, prior to a 10  $\mu\text{l}$  addition of log concentrations of Leu<sup>8</sup>-OT and Pro<sup>8</sup>-OT. Cells were excited at 530 nm and emission was recorded at 565 nm at 2-second intervals for an additional 200 seconds.

To ensure the veracity of comparisons of  $\text{EC}_{50}$  and maximum response achievable ( $\text{E}_{\text{max}}$ ) values of OT variants, all compounds were evaluated in parallel on the same 96-well plate, with the same split of cells and with identical reagent solutions. This experimental design was used for all OT peptide comparisons throughout this study, using both hOTR- and mOTR-expressing cells. Inasmuch as all assays were performed in the same CHO cell line, we can exclude differences in cellular context as a source of observed differences in peptide potency or efficacy.

To assess the role  $\text{G}_{i/o}$  in OT ligand-induced membrane hyperpolarization, cells were incubated overnight with PTX to inactivate  $\text{G}_{i/o}$  (Zhou et al., 2007). Cells were plated at 125,000 cells/ml in 96-well plates. PTX (150 ng/ml) was added 24 hours after plating and incubated for an additional 24 hours. The membrane potential assay was performed as described above. To confirm the influence of PTX on a known  $\text{G}_{i/o}$ -mediated response, the effect of PTX on  $\kappa\text{OR}$ -mediated hyperpolarization was used as a positive control (Murthy and Makhlof, 1996).  $\kappa\text{OR}$ -CHO cells were used for these experiments. The PTX assays were performed as described above for mOTR- and hOTR-expressing CHO cells, except for stimulation with dynorphin rather than OT analogs.

M119K is a  $\text{G}\beta\gamma$  inhibitor (Kirui et al., 2010). If Leu<sup>8</sup>-OT ligand-induced membrane hyperpolarization of cells is partially mediated by downstream  $\text{G}\beta\gamma$  activation of G protein-coupled inwardly rectifying potassium channels (GIRKs), then it should be partially sensitive to M119K. Cells were incubated at 37°C in 5%  $\text{CO}_2$  and 95% humidity for 35 minutes prior to a 10  $\mu\text{l}$  addition of M119K. Cells were incubated for an additional 10 minutes after drug addition. Membrane potential assays were performed as described above.

To assess potential OT ligand-induced membrane hyperpolarization through  $\text{Ca}^{2+}$ -activated potassium channels, we tested four inhibitors targeting distinct  $\text{Ca}^{2+}$ -activated potassium channel subtypes.

$\text{G}_q$ -mediated activation of protein kinase C causes an increase in cytosolic calcium (Ritter and Hall, 2009) with attendant activation of  $\text{Ca}^{2+}$ -sensitive potassium channels.  $\text{Ca}^{2+}$ -activated potassium channels are separated into three subtypes of large ( $\text{BK}_{\text{Ca}}$ ), intermediate ( $\text{IK}_{\text{Ca}}$ ), and small ( $\text{SK}_{\text{Ca}}$ ) conductance channels (Vergara et al., 1998). Paxilline is a selective inhibitor of the  $\text{BK}_{\text{Ca}}$  channel (Sanchez and McManus, 1996), whereas charybdotoxin is an inhibitor of various  $\text{IK}_{\text{Ca}}$  (Anderson et al., 1988; Ishii et al., 1997) and  $\text{BK}_{\text{Ca}}$  (Qiu et al., 2009) channels. TRAM-34 is a selective inhibitor of  $\text{IK}_{\text{Ca}}$  channel  $\text{K}_{\text{Ca}3.1}$ , which has been shown to reach maximum blockade in 3–6 minutes (Nguyen et al., 2017; Staal et al., 2017). In COS-7 cells, 100 nM TRAM-34 blocked ~90% of  $\text{IK}_{\text{Ca}}$  currents (Wulff et al., 2000). Apamin is a selective inhibitor of  $\text{SK}_{\text{Ca}}$  channels (Blatz and Magleby, 1986; Lamy et al., 2010). In human embryonic kidney (HEK) cells expressing  $\text{SK}_{\text{Ca}}$  channels  $\text{K}_{\text{Ca}2.2}$  and  $\text{K}_{\text{Ca}2.3}$ , the addition of 100 nM concentrations of apamin blocked ~70% and 80% of  $\text{K}_{\text{Ca}2.2}$ - and  $\text{K}_{\text{Ca}2.3}$ -mediated currents (Lamy et al., 2010). Cells were incubated at 37°C in 5%  $\text{CO}_2$  and 95% humidity for 35 minutes prior to a 10  $\mu\text{l}$  addition of charybdotoxin, paxilline, TRAM-34, and/or apamin. Cells were incubated for an additional 10 minutes after drug addition. Membrane potential assays were performed as described above.

NS-1619 is a  $\text{BK}_{\text{Ca}}$  channel activator (Edwards, et al., 1994; Lee et al., 1995). NS-1619 (30  $\mu\text{M}$ ) opens  $\text{BK}_{\text{Ca}}$  channels in horizontal cells of rats and mice (Sun et al., 2017). If changes in intracellular calcium are responsible for activation of the  $\text{BK}_{\text{Ca}}$ , the response should be NS-1619 sensitive. Cells were incubated at 37°C in 5%  $\text{CO}_2$  and 95% humidity for 35 minutes prior to a 10  $\mu\text{l}$  addition of paxilline. Cells were incubated for an additional 10 minutes after the paxilline addition. Membrane potential assays were performed as described above, with the exception of challenge with NS-1619 rather than OT analogs.

SKA-31 is an activator of  $\text{IK}_{\text{Ca}}$  channel  $\text{K}_{\text{Ca}3.1}$  (Sankaranarayanan et al., 2009; Christophersen and Wulff, 2015). If changes in intracellular calcium are responsible for the activation of  $\text{K}_{\text{Ca}3.1}$ , the response should be SKA-31 sensitive. Cells were incubated at 37°C in 5%  $\text{CO}_2$  and 95% humidity for 35 minutes prior to a 10  $\mu\text{l}$  addition of TRAM-34. Cells were incubated for an additional 10 minutes after TRAM-34 addition. Membrane potential assays were performed as described above, with the exception of stimulation with SKA-31 rather than OT analogs.

BAPTA-AM is an intracellular calcium chelator (Strayer et al., 1999). If changes in intracellular calcium are responsible for activation of the  $\text{Ca}^{2+}$ -activated potassium channels, the response should be BAPTA-AM sensitive. Cells were incubated at 37°C in 5%  $\text{CO}_2$  and 95% humidity for 35 minutes prior to a 10  $\mu\text{l}$  addition of BAPTA-AM. Cells were incubated for an additional 10 minutes after drug addition.

Thapsigargin was used to assess the role of intracellular calcium in OT ligand-induced changes in membrane potential. Cells were incubated at 37°C in 5%  $\text{CO}_2$  and 95% humidity for 40 minutes prior to a 10  $\mu\text{l}$  addition of thapsigargin. Cells were incubated for an additional 5 minutes after drug addition.

**Statistical Analysis.** All concentration-response data were analyzed and graphs were generated using GraphPad Prism software.  $\text{EC}_{50}$  and  $\text{E}_{\text{max}}$  values for OT peptide-stimulated increases in Fluo-3 fluorescence or decreases in FMP blue fluorescence were determined by nonlinear regression least-squares fitting of a logistic equation to the peptide concentration versus fluorescence area under the curve data. The 95% confidence intervals (CIs) for all  $\text{EC}_{50}/\text{IC}_{50}$  and  $\text{E}_{\text{max}}$  values were used to assess differences in potency and efficacy.  $R^2$  was used to assess goodness of fit. A one-way ANOVA was performed with Sidek multiple comparisons to determine statistical significance and the adjusted  $P$  values are reported.

## Results

**OT Analogs Induce  $\text{G}_q$ -Mediated Intracellular Calcium Mobilization.**  $\text{G}_q$  mediates intracellular calcium mobilization by activation of phospholipase C (PLC)  $\beta$  with

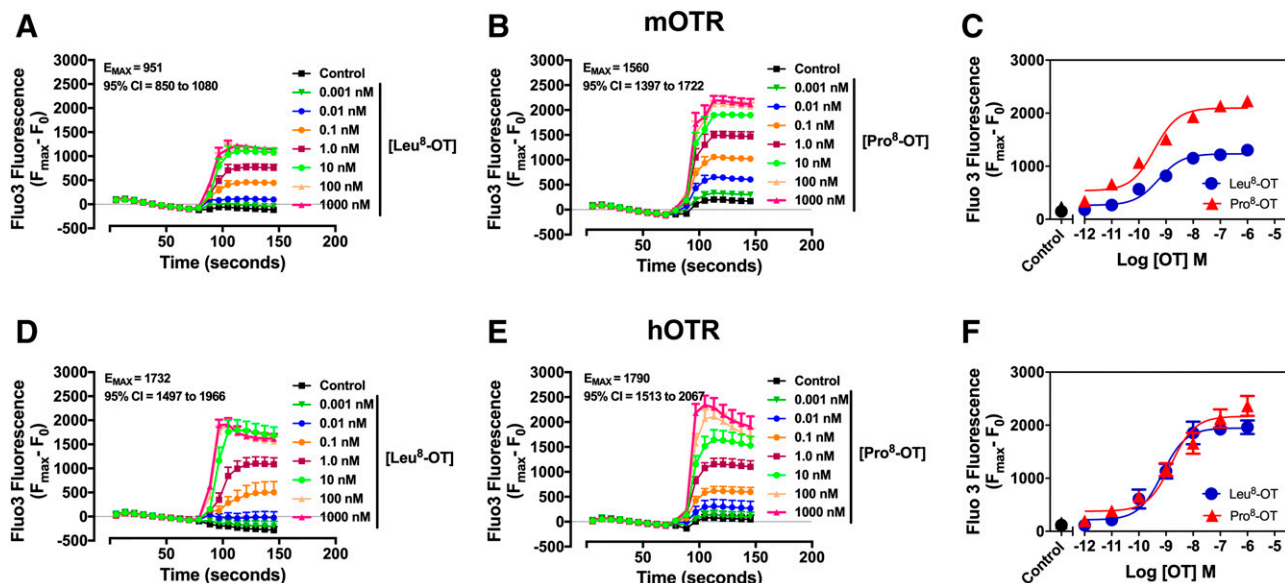


**Fig. 1.** Leu<sup>8</sup>-OT- and Pro<sup>8</sup>-OT-induced intracellular calcium mobilization in mOTR- or hOTR-expressing CHO cells. (A–C) Leu<sup>8</sup>-OT time-response (A), Pro<sup>8</sup>-OT time-response (B), and concentration-response (C) relationships in mOTR cells. (D–F) Leu<sup>8</sup>-OT time-response (D), Pro<sup>8</sup>-OT time-response (E), and concentration-response (F) relationships in hOTR cells.  $n = 6$  experiments (five replicates per concentration per experiment).

attendant inositol phosphate and diacylglycerol production (Ritter and Hall, 2009). To assess OTR activation of  $G_q$ , functional assays were performed using Fluo-3 AM as a calcium indicator dye. We asked whether Leu<sup>8</sup>-OT, found in most mammals, and Pro<sup>8</sup>-OT, found in many NWMs, show differential mobilization of intracellular  $Ca^{2+}$  upon activation of mOTRs. In mOTR CHO cells, we found that the two OT ligands produced a concentration-dependent elevation of intracellular calcium with similar potencies ( $EC_{50}$ ), but the cognate ligand Pro<sup>8</sup>-OT was more efficacious ( $E_{max}$ ) than Leu<sup>8</sup>-OT (Fig. 1, A–C; Table 1). In contrast, we found that the two OT ligands showed similar potencies and efficacies in increasing intracellular calcium concentration in hOTR CHO cells (Fig. 1, D–F; Table 1). The absence of a Leu<sup>8</sup>-OT effect on calcium concentration in nontransfected CHO-K1 cells demonstrated that the OT peptide effects observed in transfected cell lines required mOTR and hOTR expression (Supplemental Fig. 1).

Thapsigargin is a potent inhibitor of SERCA, which is responsible for maintaining the gradient between the low calcium cytosol and the sarco/endoplasmic reticulum high calcium storage. Inhibition of the SERCA pump results in a depletion of intracellular calcium stores (Dravid and Murray, 2004; Quynh Doan and Christensen, 2015). To confirm the role of intracellular calcium stores in OT-mediated calcium influx, cells were pretreated with thapsigargin. In control mOTR and hOTR CHO cells, Leu<sup>8</sup>-OT and Pro<sup>8</sup>-OT again produced concentration-dependent increases in intracellular calcium; however, pretreatment with thapsigargin abrogated this response in CHO cells expressing both mOTR and hOTR for both OT analogs (Supplemental Fig. 2). Together these data demonstrated that intracellular calcium stores represent the source of OT-mediated elevation of cytosolic calcium levels.

**OT Analog-Induced Changes in Membrane Potential Are Dependent on  $G_q$ -Mediated Calcium Mobilization.** OT analog activation of OTR and coupling to  $G_i$  have been shown to stimulate  $K^+$  channel conductances with attendant

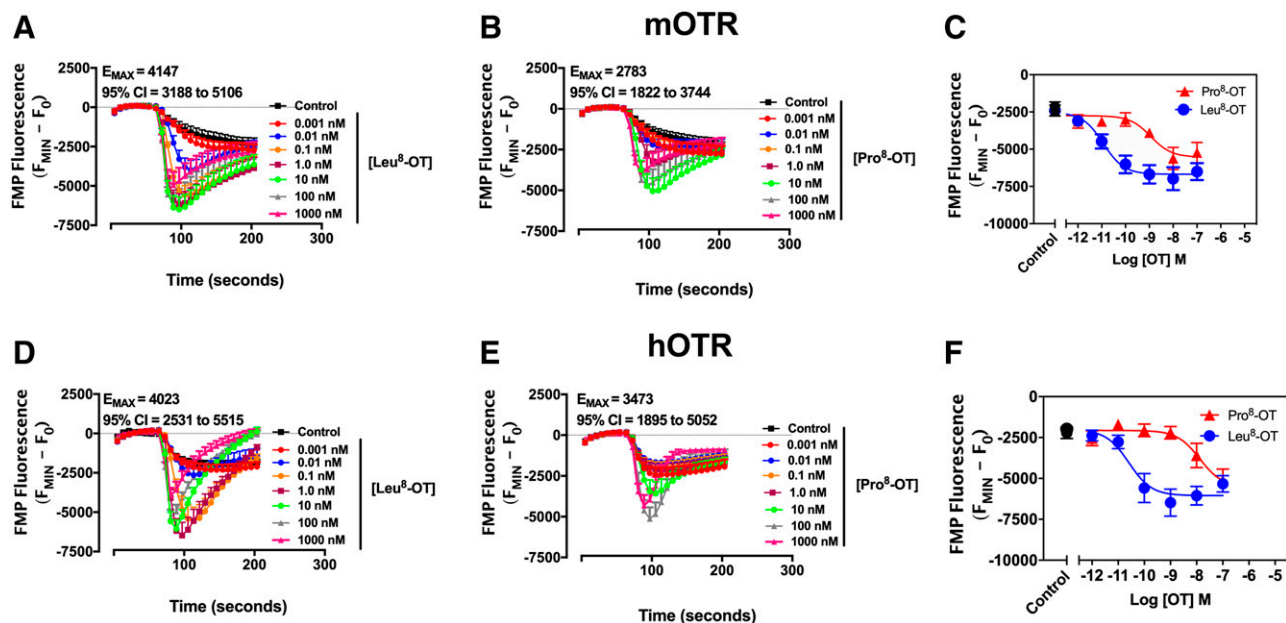
cellular hyperpolarization (Phaneuf et al., 1993; Ritter and Hall, 2009; Gravati et al., 2010). To assess potential OTR activation of  $K^+$  channel conductance, we performed functional assays using the membrane potential-sensitive dye, FMP blue. FMP blue dye is a lipophilic, anionic, bis-oxonol-based dye that distributes across the cell membrane as a function of membrane potential and displays depolarization-induced increased fluorescence emission after binding to intracellular proteins or decreased fluorescence after hyperpolarization-induced egress from cells (Whiteaker et al., 2001; Baxter et al., 2002). In mOTR CHO cells, both Leu<sup>8</sup>-OT and Pro<sup>8</sup>-OT produced concentration-dependent decreases in FMP blue fluorescence consistent with a hyperpolarization response. Leu<sup>8</sup>-OT showed substantially greater potency compared with Pro<sup>8</sup>-OT in the observed changes in membrane potential, with the two OT ligands showing comparable efficacies (Fig. 2, A–C; Table 2). A similar pattern was observed in hOTR CHO cells, with Leu<sup>8</sup>-OT displaying greater potency than Pro<sup>8</sup>-OT with regard to changes in membrane potential (Fig. 2, D–F; Table 2). The absence of Leu<sup>8</sup>-OT and Pro<sup>8</sup>-OT effects on membrane potential in nontransfected CHO-K1 cells again demonstrated the requirement for mOTR

TABLE 1

Potency of Leu<sup>8</sup>-OT and Pro<sup>8</sup>-OT at inducing calcium mobilization in mOTR and hOTR CHO cells

Parameter	Ligand		Rank Order Potency
	Leu <sup>8</sup> -OT	Pro <sup>8</sup> -OT	
	<i>nM</i>		
mOTR			
$EC_{50}$	0.5	0.4	Pro <sup>8</sup> -OT = Leu <sup>8</sup> -OT
95% CI	0.3–1.0	0.2–0.7	
$R^2$	0.90	0.92	
hOTR			
$EC_{50}$	0.7	1.6	Leu <sup>8</sup> -OT = Pro <sup>8</sup> -OT
95% CI	0.4–1.5	0.7–3.6	
$R^2$	0.87	0.84	





**Fig. 2.** Leu<sup>8</sup>-OT- and Pro<sup>8</sup>-OT-induced changes in membrane potential in mOTR- or hOTR-expressing CHO cells. (A–C) Leu<sup>8</sup>-OT time-response (A), Pro<sup>8</sup>-OT time-response (B), and concentration-response (C) relationships in mOTR cells. (D–F) Leu<sup>8</sup>-OT time-response (D), Pro<sup>8</sup>-OT time-response (E), and concentration-response (F) relationships in hOTR cells.  $n = 6$  experiments (five replicates per dose per experiment).

and hOTR transfection in the observed hyperpolarization responses to OT ligands (Supplemental Fig. 3).

Several classes of G-protein  $\alpha$  subunits, including G<sub>i</sub> and G<sub>o</sub>, can be mono-ADP-ribosylated by the exotoxin from the Gram-negative bacterium *Bordetella pertussis*. PTX catalyzes the covalent transfer of an ADP-ribose from NAD<sup>+</sup> to a cysteine residue four amino acids from the carboxy termini of these  $\alpha$  subunits (Murray and Siebenaller, 1993). This ADP-ribosylation disrupts the coupling between GPCRs and PTX-sensitive G proteins and therefore potentially interferes with responses to agonists such as OT. We tested mOTR CHO cells and observed that PTX treatment partially affected Leu<sup>8</sup>-OT-mediated hyperpolarization, with a significant 31.9% reduction in efficacy. The Leu<sup>8</sup>-OT  $E_{max}$  was 3590 (95% CI, 3088–4093) in control cells compared with 2446 in PTX-pretreated cells (95% CI, 1893–2999) (Fig. 3A; Supplemental Fig. 4, A and C). In contrast, pretreatment with PTX did not significantly inhibit Leu<sup>8</sup>-OT-mediated hyperpolarization in hOTR CHO cells (Fig. 3C; Supplemental Fig. 4, E and G; Supplemental Table 1). PTX treatment did not affect Pro<sup>8</sup>-OT-induced hyperpolarization in either mOTR-expressing (Fig. 3B; Supplemental Fig. 4, B and D) or hOTR CHO cells (Fig. 3D; Supplemental Fig. 4, F and H). These data demonstrate that in mOTR CHO cells, Leu<sup>8</sup>-OT-induced hyperpolarization is partially sensitive to PTX. The insensitivity of Pro<sup>8</sup>-OT to PTX in mOTR and hOTR CHO cells indicates a lack of involvement of G<sub>i</sub>-mediated activation of GIRKs in the observed changes in membrane potential. In contrast, the partial sensitivity of Leu<sup>8</sup>-OT-induced changes in membrane potential in mOTR-expressing cells suggests that both G<sub>i</sub>-mediated and PTX-insensitive pathways are involved in the hyperpolarization in response to this peptide.

We used a  $\kappa$ OR-CHO cell line as a positive control to demonstrate the ability of PTX to disrupt G-protein coupling to a GPCR.  $\kappa$ ORs couple to the PTX substrate G<sub>i</sub>. Dynorphin A 1-13-NH<sub>2</sub> was used as the  $\kappa$ OR agonist for these experiments.

Dynorphin A 1-13-NH<sub>2</sub> produced a robust hyperpolarization response in control  $\kappa$ OR-CHO cells, and this response was abrogated in PTX-pretreated cells (Supplemental Fig. 5). These data demonstrate the effectiveness of PTX in disrupting GPCR coupling to G<sub>i</sub>.

PTX disrupts GPCR interaction with sensitive G proteins, thereby interrupting downstream G $\alpha$ - and G $\beta\gamma$ -dependent signaling. To further assess the partial G<sub>i</sub> mediation of Leu<sup>8</sup>-OT-induced changes in membrane potential in mOTR CHO cells, the G $\beta\gamma$  inhibitor M119K was used. M119K binds to G $\beta\gamma$  with high affinity, and in vitro studies demonstrate that it inhibits G $\beta\gamma$  function (Bonacci et al., 2006; Kirui et al., 2010). G $\beta\gamma$  subunits can directly activate GIRK channels, and reassociation with the G $\alpha$  subunit terminates this signaling (Petit-Jacques et al., 1999; Lin and Smrcka, 2011). In mOTR and hOTR CHO cells, pretreatment with M119K did not produce a statistically significant reduction in Leu<sup>8</sup>-OT-induced membrane hyperpolarization (Supplemental Fig. 6; Supplemental Table 2). Together, these data suggest that in mOTR-expressing cells, but not hOTR CHO cells, Leu<sup>8</sup>-OT modulation of membrane

TABLE 2

Potency of Leu<sup>8</sup>-OT and Pro<sup>8</sup>-OT at inducing membrane hyperpolarization in mOTR and hOTR CHO cells

Parameter	Ligand		Rank Order Potency
	Leu <sup>8</sup> -OT	Pro <sup>8</sup> -OT	
	$\mu$ M	nM	
mOTR			
EC <sub>50</sub>	11.6	1.1	Leu <sup>8</sup> -OT > Pro <sup>8</sup> -OT
95% CI	3.1–47.3	0.2–5.6	
R <sup>2</sup>	0.71	0.53	
hOTR			
EC <sub>50</sub>	25.6	13.23	Leu <sup>8</sup> -OT > Pro <sup>8</sup> -OT
95% CI	4.4–150.0	2.4–73.6	
R <sup>2</sup>	0.53	0.54	

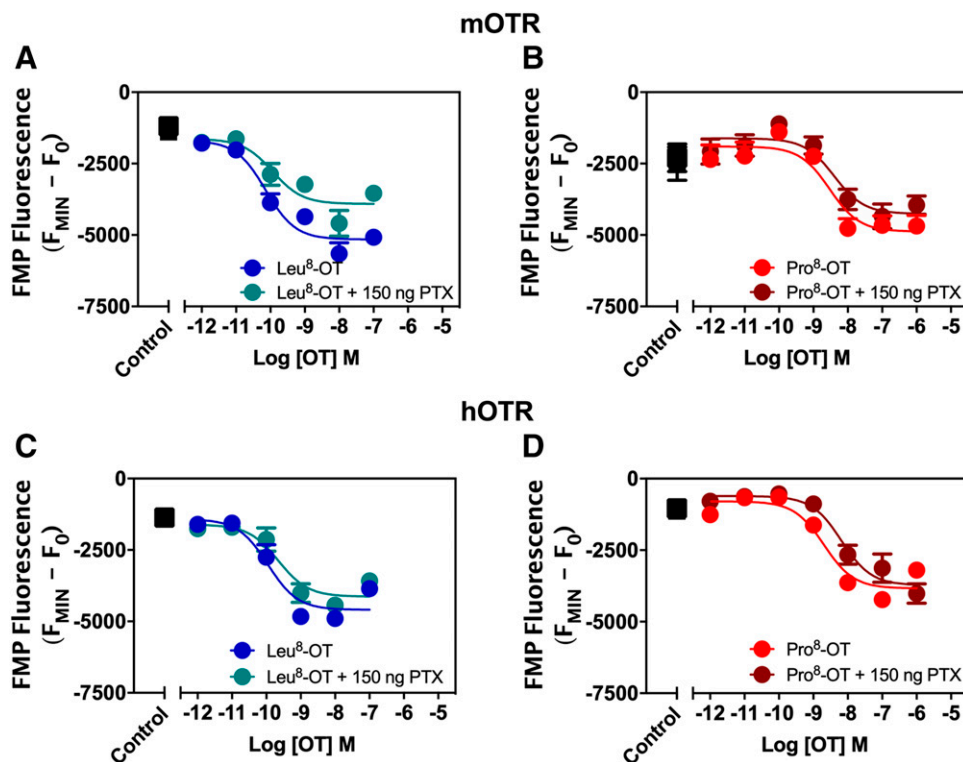


**Fig. 3.** Effects of pretreatment with PTX on Leu<sup>8</sup>-OT- and Pro<sup>8</sup>-OT-induced changes in membrane potential in mOTR- and hOTR-expressing CHO cells. (A and B) Control Leu<sup>8</sup>-OT and PTX-pretreated concentration-response relationships (A) and control Pro<sup>8</sup>-OT and PTX-pretreated concentration-response relationships (B) in mOTR-expressing cells. (C and D) Control Leu<sup>8</sup>-OT and PTX-pretreated concentration-response relationships (C) and control Pro<sup>8</sup>-OT and PTX-pretreated concentration-response relationships (D) in hOTR-expressing cells. Control and PTX-pretreated replicates were run in parallel on the same plates, at the same time and with the same split of cells.  $n = 6$  experiments (five replicates per dose per experiment).

potential is partially mediated by GIRK channels, but a role for  $G\beta\gamma$ -dependent signaling was not established.

Given that Pro<sup>8</sup>-OT-induced changes in membrane potential were insensitive to PTX and Leu<sup>8</sup>-OT-induced changes were only partially sensitive in mOTR-expressing cells, we next considered the possibility that OT peptide-induced hyperpolarization may involve coupling to  $G_q$  with activation of PLC $\beta$  and calcium-dependent  $K^+$  channel activation. To explore the role of  $Ca^{2+}$ -activated  $K^+$  channels in OT analog-induced changes in membrane potential, we used a pharmacological approach with compounds that discriminate between subtypes of  $Ca^{2+}$ -activated  $K^+$  channels. To assess the role of SK<sub>Ca</sub> channels in OT-mediated membrane hyperpolarization in mOTR and hOTR cells, cells were pretreated with the SK<sub>Ca</sub>-selective blocker apamin. Molecular modeling and mutational studies suggest that apamin functions to block SK<sub>Ca</sub> channels through an allosteric mechanism rather than a classic pore block (Lamy et al., 2010). In mOTR and hOTR CHO cells, apamin produced very modest inhibition of Leu<sup>8</sup>-OT-induced changes (16.4% and 6.6%, respectively) (Fig. 4, A and C; Supplemental Figs. 7A and 8A, Supplementary Table 3) and did not affect Pro<sup>8</sup>-OT-induced changes in membrane potential (Fig. 4, B and D; Supplemental Figs. 7B and 8B, Supplementary Table 3). To confirm that OT-analog vehicle DMSO (0.02%) and apamin solvent acetic acid (5  $\mu$ M) did not affect membrane hyperpolarization, additional controls of DMSO vehicle and acetic acid solvent were performed. Neither DMSO nor acetic acid vehicles alone affected membrane potential in mOTR- and hOTR-expressing cells (Supplemental Fig. 9). These data indicate that the acetic acid vehicle did not substantially affect membrane hyperpolarization and that SK<sub>Ca</sub> channels provide minimal contribution to OT analog-induced changes in membrane potential in either mOTR- or hOTR-expressing CHO cells.

Charybdotoxin exhibits blocking effects on both IK<sub>Ca</sub> and BK<sub>Ca</sub> (Anderson et al., 1988; MacKinnon and Miller, 1988; Ishii et al., 1997; Qiu et al., 2009). Charybdotoxin binds to the BK<sub>Ca</sub> channel in either the open or closed conformation and dissociation from the BK<sub>Ca</sub> channel is voltage dependent (MacKinnon and Miller, 1988). In mOTR CHO cells, charybdotoxin did not affect changes in membrane potential produced by either Leu<sup>8</sup>-OT (Fig. 4A; Supplemental Fig. 7C, Supplementary Table 3) or Pro<sup>8</sup>-OT (Fig. 4B; Supplemental Fig. 7D, Supplementary Table 3); however, in hOTR CHO cells, charybdotoxin modestly reduced Leu<sup>8</sup>-OT- and Pro<sup>8</sup>-OT-induced hyperpolarization by 17.0% (Fig. 4C; Supplemental Fig. 8C, Supplementary Table 3) and 24.3% (Fig. 4D; Supplemental Fig. 8D, Supplementary Table 3), respectively. These results suggested that IK<sub>Ca</sub> and/or BK<sub>Ca</sub> channels may partially contribute to OT-mediated changes in membrane potential. To further assess the role of BK<sub>Ca</sub> channels, mOTR and hOTR cells were pretreated with the BK<sub>Ca</sub> blocker paxilline. Paxilline produces inhibition by stabilizing the BK<sub>Ca</sub> channels in the closed conformation (Zhou and Lingle, 2014). In mOTR CHO cells, paxilline did not affect Leu<sup>8</sup>-OT-induced changes in membrane potential (Fig. 4A; Supplemental Fig. 7C, Supplementary Table 3), whereas the Pro<sup>8</sup>-OT response was reduced by 40.5% (Fig. 4B; Supplemental Fig. 7D, Supplementary Table 3). In hOTR CHO cells, paxilline modestly inhibited hyperpolarization by both Leu<sup>8</sup>-OT (20.6%) (Fig. 4C; Supplemental Fig. 8C, Supplementary Table 3) and Pro<sup>8</sup>-OT (26.5%) (Fig. 4D; Supplemental Fig. 8D, Supplementary Table 3), suggesting that BK<sub>Ca</sub> channels do contribute to OT-mediated changes in membrane potential by hOTR. To confirm the involvement of BK<sub>Ca</sub> channels in hyperpolarization of mOTR and hOTR CHO cells, we next used the BK<sub>Ca</sub> activator NS-1619. In mOTR and hOTR CHO cells, paxilline inhibited NS-1619-induced membrane

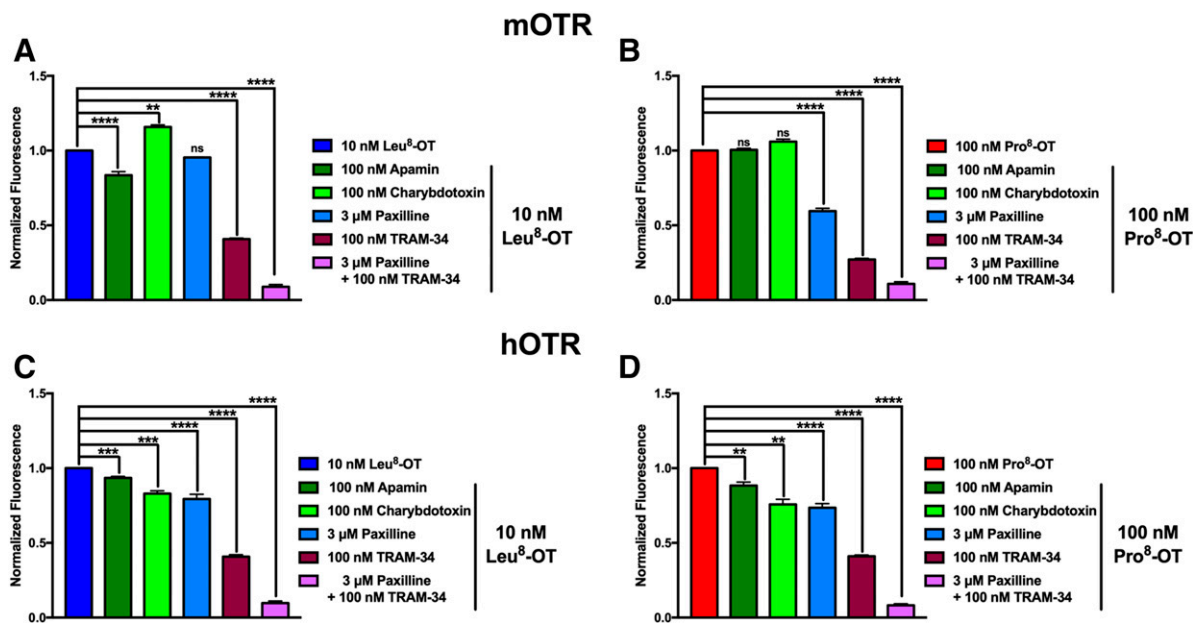


**Fig. 4.** Effects of pretreatment with  $\text{Ca}^{2+}$ -activated  $\text{K}^+$  inhibitors on  $\text{Leu}^{\text{S-OT}}$ - or  $\text{Pro}^{\text{S-OT}}$ -induced changes in membrane potential in mOTR- and hOTR-expressing CHO cells. Inhibitor fluorescence was normalized to  $\text{Leu}^{\text{S-OT}}$ - or  $\text{Pro}^{\text{S-OT}}$ -induced membrane hyperpolarization. (A) In mOTR-expressing cells,  $\text{Leu}^{\text{S-OT}}$  (blue) relative fluorescence is compared to pretreatment with  $\text{SK}_{\text{Ca}}$  inhibitor apamin (green),  $\text{BK}_{\text{Ca}}$  and  $\text{IK}_{\text{Ca}}$  inhibitor charybdotoxin (fluorescent green),  $\text{BK}_{\text{Ca}}$  inhibitor paxilline (light blue),  $\text{IK}_{\text{Ca}}$  inhibitor TRAM-34 (maroon) and  $\text{BK}_{\text{Ca}}$  and  $\text{IK}_{\text{Ca}}$  inhibitors paxilline plus TRAM-34 (lavender). (B) In mOTR-expressing cells,  $\text{Pro}^{\text{S-OT}}$  (red) relative fluorescence is compared to pretreatment with  $\text{SK}_{\text{Ca}}$  inhibitor apamin (green),  $\text{BK}_{\text{Ca}}$  and  $\text{IK}_{\text{Ca}}$  inhibitor charybdotoxin (fluorescent green),  $\text{BK}_{\text{Ca}}$  inhibitor paxilline (light blue),  $\text{IK}_{\text{Ca}}$  inhibitor TRAM-34 (maroon) and  $\text{BK}_{\text{Ca}}$  and  $\text{IK}_{\text{Ca}}$  inhibitors paxilline plus TRAM-34 (lavender). (C) In hOTR-expressing cells,  $\text{Leu}^{\text{S-OT}}$  (blue) relative fluorescence is compared to pretreatment with  $\text{SK}_{\text{Ca}}$  inhibitor apamin (green),  $\text{BK}_{\text{Ca}}$  and  $\text{IK}_{\text{Ca}}$  inhibitor charybdotoxin (fluorescent green),  $\text{BK}_{\text{Ca}}$  inhibitor paxilline (light blue),  $\text{IK}_{\text{Ca}}$  inhibitor TRAM-34 (maroon) and  $\text{BK}_{\text{Ca}}$  and  $\text{IK}_{\text{Ca}}$  inhibitors paxilline plus TRAM-34 (lavender). (D) In hOTR-expressing cells,  $\text{Pro}^{\text{S-OT}}$  (red) relative fluorescence is compared to pretreatment with  $\text{SK}_{\text{Ca}}$  inhibitor apamin (green),  $\text{BK}_{\text{Ca}}$  and  $\text{IK}_{\text{Ca}}$  inhibitor charybdotoxin (fluorescent green),  $\text{BK}_{\text{Ca}}$  inhibitor paxilline (light blue),  $\text{IK}_{\text{Ca}}$  inhibitor TRAM-34 (maroon) and  $\text{BK}_{\text{Ca}}$  and  $\text{IK}_{\text{Ca}}$  inhibitors paxilline plus TRAM-34 (lavender). Area under the curve (negative peaks only) was assessed and a one-way ANOVA was performed with Sidak multiple comparisons to determine statistical significance.  $n = 3$  experiments for each inhibitor (10 replicates per dose per experiment). Raw data are shown in Supplemental Figs. 7 and 8. Adjusted  $P$  values are presented in Supplemental Table 3 and significance is indicated by asterisks in this figure.

hyperpolarization in a concentration-dependent manner, with a  $30 \mu\text{M}$  paxilline concentration inhibiting the response by 77.8% and 79.0%, respectively (Supplemental Fig. 10, A, B, E, and F, Supplementary Table 4), confirming a role for  $\text{BK}_{\text{Ca}}$  channels in the regulation of CHO cell membrane potential.

TRAM-34 is an  $\text{IK}_{\text{Ca}}$   $\text{K}^+$  channel blocker that specifically blocks  $\text{K}_{\text{Ca}3.1}$  by occupying the site that  $\text{K}^+$  binds to before entering the selectivity filter (Nguyen et al., 2017). TRAM-34 produced the most robust inhibition of OT-mediated changes in membrane potential. In mOTR CHO cells, TRAM-34 inhibited the  $\text{Leu}^{\text{S-OT}}$  response by 59.2% (Fig. 4A; Supplemental Fig. 7E, Supplementary Table 3) and the  $\text{Pro}^{\text{S-OT}}$  response by 72.9% (Fig. 4B; Supplemental Fig. 7F, Supplementary Table 3). Similarly, in hOTR CHO cells, TRAM-34 inhibited  $\text{Leu}^{\text{S-OT}}$  by 59.2% (Fig. 4C; Supplemental Fig. 8E, Supplementary Table 3) and  $\text{Pro}^{\text{S-OT}}$  by 58.9% (Fig. 4D; Supplemental Fig. 8F, Supplementary Table 3). To confirm participation of  $\text{K}_{\text{Ca}3.1}$  channels in the regulation of membrane potential in mOTR- and hOTR-expressing cells, we next challenged cells with the  $\text{K}_{\text{Ca}3.1}$  activator SKA-31. In mOTR and hOTR CHO cells, TRAM-34 inhibited SKA-31-induced membrane hyperpolarization in a concentration-dependent manner, with 300 nM inhibiting the response by 73.4% and 91.5%, respectively (Supplemental Fig. 10, C, D, G, and H, Supplementary Table 4). These data document an important role for  $\text{K}_{\text{Ca}3.1}$  as a mediator of the response to OTR-driven  $\text{Ca}^{2+}$ -dependent hyperpolarization in mOTR- and

hOTR-expressing CHO cells. To demonstrate the combined contribution of  $\text{BK}_{\text{Ca}}$  and  $\text{K}_{\text{Ca}3.1}$  channels in the observed OT-mediated changes in membrane potential, cells were pretreated with both paxilline and TRAM-34. In mOTR and hOTR CHO cells, the combined exposure of paxilline and TRAM-34 inhibited both  $\text{Leu}^{\text{S-OT}}$ - and  $\text{Pro}^{\text{S-OT}}$ -induced hyperpolarization by ~85% (Fig. 4; Supplemental Figs. 7, G and H and 8, G and H, Supplementary Table 3), indicating an additive effect. These data confirm that  $\text{BK}_{\text{Ca}}$  and  $\text{IK}_{\text{Ca}}$  channels are largely responsible for OT-induced changes in membrane potential.

To directly assess the role of calcium in OT-mediated membrane hyperpolarization, cells were pretreated with the intracellular calcium chelator BAPTA-AM. In both mOTR and hOTR CHO cells, BAPTA-AM exposure blocked hyperpolarization of membrane potential with either  $\text{Leu}^{\text{S-OT}}$  or  $\text{Pro}^{\text{S-OT}}$  (Supplemental Fig. 11, A, B, E, and F). Interestingly, in BAPTA-AM-treated hOTR CHO cells, a  $\text{Leu}^{\text{S-OT}}$ -induced depolarization was observed (Supplemental Fig. 11E), indicating a possible dual modulation of  $\text{K}^+$  channel currents by the OTR (Gravati et al., 2010).

We next confirmed the role of intracellular calcium stores in OT-mediated changes in membrane potential by pretreating cells with thapsigargin and measuring membrane potential responses to OT analogs in mOTR and hOTR CHO cells. As expected, pretreatment with thapsigargin eliminated hyperpolarization produced by either  $\text{Leu}^{\text{S-OT}}$

(Supplemental Fig. 11, C and G) or Pro<sup>8</sup>-OT (Supplemental Fig. 11, D and H). Interestingly, in thapsigargin-pretreated hOTR CHO cells, Leu<sup>8</sup>-OT and Pro<sup>8</sup>-OT both produced a depolarization response (Supplemental Fig. 11, G and H), again indicating potential dual modulation of currents by the hOTR.

## Discussion

Previous studies demonstrated promiscuous activation of various G proteins by OT peptides in a variety of cell types (Phaneuf et al., 1993; Reversi et al., 2005; Gravati et al., 2010; Busnelli et al., 2012, 2016; Parreiras-e-Silva et al., 2017). In this study, we compared a natural variation in OT ligands in mOTR- and hOTR-expressing CHO cells to assess downstream activation of G-protein signaling pathways. Our findings initially confirmed that at both the mOTR and hOTR, Leu<sup>8</sup>-OT and Pro<sup>8</sup>-OT activated G<sub>q</sub> signaling in a concentration-dependent manner resulting in an increase in intracellular calcium concentration. Notably, in mOTR CHO cells, the cognate ligand Pro<sup>8</sup>-OT was more efficacious than Leu<sup>8</sup>-OT, which may reflect ligand-receptor coevolutionary changes observed in NWMs (Ren et al., 2015). Alignment using the National Center for Biotechnology Information Basic Local Alignment Search Tool indicates that human and marmoset (*Callithrix jacchus*) OTRs are 94% conserved (Boratyn et al., 2012). OT ligands interact with the three-dimensional environment of the extracellular region and transmembrane domains. Amino acid changes are considered radical or conservative based on the magnitude of their physiochemical differences. There are 20 amino acid changes between hOTRs and mOTRs, six of which are located in the extracellular and transmembrane regions (Ren et al., 2015; Supplemental Table 5), that may affect ligand binding. The increased efficacy observed with Pro<sup>8</sup>-OT in mOTR CHO cells may contribute to sociobehavioral responses in marmosets. In contrast to the superior efficacy of Pro<sup>8</sup>-OT in the calcium mobilization assay at the mOTR, no significant differences in efficacy were observed between Pro<sup>8</sup>-OT and Leu<sup>8</sup>-OT using the same assay in hOTR CHO cells. Similarly, no significant differences in the potency of either Leu<sup>8</sup>-OT or Pro<sup>8</sup>-OT were observed in the Ca<sup>2+</sup> mobilization assay in mOTR and hOTR CHO cells. The observed EC<sub>50</sub> values were consistent with those found previously in hOTR-expressing cell lines (Busnelli et al., 2012; Parreiras-e-Silva et al., 2017), and they were comparable to results from hOTR-expressing HEK cells in which Leu<sup>8</sup>-OT, Pro<sup>8</sup>-OT, and Val<sup>3</sup>-Pro<sup>8</sup>-OT function as full agonists at a G<sub>q</sub> signaling pathway (Parreiras-e-Silva et al., 2017). The results of these previous studies with hOTR were extended in this investigation by comparing mOTR and hOTR signaling responses.

Given a previous report that Leu<sup>8</sup>-OT exerts a dual modulation of inward rectifier K<sup>+</sup> currents in olfactory neuronal cells (Gravati et al., 2010), we next assessed the ability of OT ligands to trigger a hyperpolarization response. GIRK channels are regulators of cellular excitability, and stimulation of a variety of GPCRs that couple to G<sub>i/o</sub> G proteins, such as the  $\mu$ -opioid receptor, activates GIRK channels via G-protein G $\beta\gamma$  subunits (Rifkin et al., 2017). Both OT ligands induced membrane hyperpolarization in mOTR- and hOTR-expressing cells in a concentration-dependent manner. The membrane-hyperpolarizing responses displayed significant OT peptide-specific differences in potency.

In both mOTR- and hOTR-expressing cells, Leu<sup>8</sup>-OT was ~100-fold more potent than Pro<sup>8</sup>-OT in inducing membrane hyperpolarization.

PTX inhibits its G<sub>α</sub> protein substrate from coupling to receptors, thus blocking G<sub>i/o</sub>-mediated responses including membrane hyperpolarization mediated by GIRK channels. The efficacy of Leu<sup>8</sup>-OT in the FMP blue assay was only modestly reduced by PTX in mOTR CHO cells. This suggested a minor G<sub>i/o</sub> and GIRK contribution to Leu<sup>8</sup>-OT-induced hyperpolarization of membrane potential. In contrast to the partial sensitivity of Leu<sup>8</sup>-OT, the Pro<sup>8</sup>-OT-induced hyperpolarization response was completely insensitive to PTX in both mOTR- and hOTR-expressing CHO cells, demonstrating a bias against G<sub>i</sub> activation. This pattern of Leu<sup>8</sup>-OT and Pro<sup>8</sup>-OT producing primary coupling of OTRs to G<sub>q</sub>, with minor activation of G<sub>i</sub> by Leu<sup>8</sup>-OT, is consistent with previous reports for these peptides in hOTR-expressing HEK293 cells (Parreiras-e-Silva et al., 2017). At the hOTR, Leu<sup>8</sup>-OT has been shown to produce a robust internalization, whereas the response to Pro<sup>8</sup>-OT was modest (Parreiras-e-Silva et al., 2017).

OT has also previously been shown to exert a dual action in olfactory GN11 cells both stimulating and inhibiting K<sup>+</sup> conductances belonging to the inward rectifier family of K<sup>+</sup> channels (Gravati et al., 2010). The OT-mediated inward rectifier current inhibition was mediated by a PTX-resistant G protein, presumably of the G<sub>q/11</sub> subtype, and by PLC activation, whereas the activation of a K<sup>+</sup> conductance was mediated by a PTX-sensitive G<sub>i/o</sub> (Gravati et al., 2010). These differences in G-protein subtype regulation of K<sup>+</sup> conductances observed previously in the GN11 cell line underscore the importance of cellular context in measurements of signaling pathways. The partial PTX sensitivity observed at the mOTR with Leu<sup>8</sup>-OT, but not Pro<sup>8</sup>-OT, appears to represent an agonist functional selectivity where the two OT ligands activate a single receptor but produce distinct signaling outcomes (Rankovic et al., 2016).

A variety of hormones and neurotransmitters acting at GPCRs are capable of producing [Ca<sup>2+</sup>]<sub>i</sub> elevation typically mediated by Ca<sup>2+</sup> release from the endoplasmic reticulum via the Gq/phosphoinositide-PLC pathway. This G<sub>q</sub> signaling pathway affords another potential mechanism for hyperpolarizing responses through activation of Ca<sup>2+</sup>-dependent potassium channels. A role for Ca<sup>2+</sup>-activated K<sup>+</sup> channels in the hyperpolarization responses observed in mOTR- and hOTR-expressing CHO cells was therefore assessed using BK<sub>Ca</sub> (K<sub>Ca</sub>1.1), IK<sub>Ca</sub> (K<sub>Ca</sub>3.1), and SK<sub>Ca</sub> channel blockers. Paxilline selectively blocks BK<sub>Ca</sub> channels, and pretreatment with this inhibitor resulted in a significant reduction in the hyperpolarization response observed with Pro<sup>8</sup>-OT in mOTR cells and the response to both Leu<sup>8</sup>-OT and Pro<sup>8</sup>-OT in hOTR-expressing cells. Paxilline also inhibited the hyperpolarizing response to the BK<sub>Ca</sub> channel opener NS-1619 in both mOTR and hOTR CHO cells, further supporting a role for a BK<sub>Ca</sub> channel contribution to the observed membrane hyperpolarization. These results agree with those of an earlier report demonstrating that Leu<sup>8</sup>-OT hyperpolarized myenteric intrinsic primary afferent neurons by activating BK<sub>Ca</sub> channels via the OTR-PLC-inositol trisphosphate-Ca<sup>2+</sup> signaling pathway (Che et al., 2012).

TRAM-34 inhibited between 58% and 73% of the hyperpolarizing responses to both OT ligands, suggesting that



K<sub>Ca</sub>3.1 is largely responsible for membrane hyperpolarization produced by OT peptides in mOTR- and hOTR-expressing CHO cells. TRAM-34 also inhibited the hyperpolarizing response to K<sub>Ca</sub>3.1 opener SKA-31, further demonstrating the involvement of K<sub>Ca</sub>3.1 in observed membrane hyperpolarization. The critical role of [Ca<sup>2+</sup>]<sub>i</sub> elevation in hyperpolarization was demonstrated using BAPTA-AM to chelate intracellular Ca<sup>2+</sup> (Strayer et al., 1999). Pretreatment with BAPTA-AM eliminated membrane hyperpolarization in response to both OT analogs in mOTR and hOTR cells. Similarly, passive depletion of endoplasmic reticulum Ca<sup>2+</sup> stores by the endoplasmic reticulum Ca<sup>2+</sup>-ATPase inhibitor, thapsigargin (Dravid and Murray, 2004; Quynh Doan and Christensen, 2015), also inhibited OT-induced membrane hyperpolarization produced by both OT analogs in both cell lines. These data confirm that the observed OT ligand-induced membrane hyperpolarization in mOTR- and hOTR-expressing CHO cells was primarily mediated by intracellular Ca<sup>2+</sup> mobilization with subsequent activation of Ca<sup>2+</sup>-dependent K<sup>+</sup> channels, including K<sub>Ca</sub>3.1.

OT is a fundamental mediator of sociobehavioral processes, including social cognition (Crespi, 2016), interpersonal trust (Kosfeld et al., 2005; Baumgartner et al., 2008), anxiety (Missig et al., 2010), and stress response (Light et al., 2000; Cavanaugh et al., 2016), generating interest in OT as a potential therapeutic mediator of sociobehavioral deficits in conditions such as autism spectrum disorder (Andari et al., 2010; Anagnostou et al., 2012), post-traumatic stress disorder (Frijling, 2017; Sack et al., 2017), and schizophrenia (Pedersen et al., 2011; Brambilla et al., 2016). One major challenge is connecting pharmacologic signatures to sociobehavioral processes. Identification of the mechanisms by which OT analogs affect OTR-mediated signaling is crucial to translating signaling activation at the cellular level to effects of OT ligands on social behaviors. In clinical trials for sociobehavioral deficits, intranasal OT is used because peripheral administration does not cross the blood-brain barrier (Born et al., 2002). Intranasal OT appears to be safe and well tolerated (Anagnostou et al., 2012) and imaging evidence suggests that OT induces increased activity in the “social brain” (Bethlehem et al., 2013). However, clinical trials for OT treatment of sociobehavioral deficits with various dosing schedules (single vs. multiple) and routes (intravenous vs. intranasal) have shown mixed results (Alvares et al., 2017), suggesting that greater understanding of OT-triggered signaling pathways downstream of the OTR could facilitate interpretation of sociobehavioral effects and lead to more refined therapeutic targeting.

These results show that Leu<sup>8</sup>-OT and Pro<sup>8</sup>-OT display functionally distinct responses when activating either the mOTR or hOTR. These distinct characteristics included peptide potency and efficacy as well as G-protein subtype coupling. Pro<sup>8</sup>-OT was shown to be more efficacious than Leu<sup>8</sup>-OT in activating the G<sub>q</sub> Ca<sup>2+</sup> mobilization assay in mOTR cells. Uniquely, Leu<sup>8</sup>-OT was much more potent than Pro<sup>8</sup>-OT in producing a hyperpolarization in both mOTR and hOTR. A final salient difference in the observed pharmacologic signatures of the two peptides was that the Pro<sup>8</sup>-OT-induced hyperpolarization responses in both mOTR and hOTR were PTX insensitive, whereas the response to Leu<sup>8</sup>-OT in mOTR was partially sensitive. Further functional characterization of OT analogs may therefore provide insight into the structural

requirements for functionally selective or biased agonists that open new possibilities for drug discovery and the advancement of OT-mediated therapeutics.

#### Acknowledgments

We thank Dr. Myron Toews for input during the planning of this project and Dr. Jack Taylor and Bridget Seifanek for careful reading of the manuscript.

#### Authorship Contributions

*Participated in research design:* Pierce, Mehrotra, Murray.  
*Conducted experiments:* Pierce, Mehrotra, Mustoe.  
*Performed data analysis:* Pierce, Mehrotra, Mustoe.  
*Wrote or contributed to the writing of the manuscript:* Pierce, Mehrotra, Mustoe, French, Murray.

#### References

- Alvares GA, Quintana DS, and Whitehouse AJ (2017) Beyond the hype and hope: critical considerations for intranasal oxytocin research in autism spectrum disorder. *Autism Res* **10**:25–41.
- Anagnostou E, Soorya L, Chaplin W, Bartz J, Halpern D, Wasserman S, Wang AT, Pepa L, Tanel N, Kushki A, et al. (2012) Intranasal oxytocin versus placebo in the treatment of adults with autism spectrum disorders: a randomized controlled trial. *Mol Autism* **3**:16.
- Andari E, Duhamel JR, Zalla T, Herbrecht E, Leboyer M, and Sirigu A (2010) Promoting social behavior with oxytocin in high-functioning autism spectrum disorders. *Proc Natl Acad Sci USA* **107**:4389–4394.
- Anderson AJ, Harvey AL, Rowan EG, and Strong PN (1988) Effects of charybdotoxin, a blocker of Ca<sup>2+</sup>-activated K<sup>+</sup> channels, on motor nerve terminals. *Br J Pharmacol* **95**:1329–1335.
- Baumgartner T, Heinrichs M, Vonlanthen A, Fischbacher U, and Fehr E (2008) Oxytocin shapes the neural circuitry of trust and trust adaptation in humans. *Neuron* **58**:639–650.
- Baxter DF, Kirk M, Garcia AF, Raimondi A, Holmqvist MH, Flint KK, Bojanic D, Distefano PS, Curtis R, and Xie Y (2002) A novel membrane potential-sensitive fluorescent dye improves cell-based assays for ion channels. *J Biomol Screen* **7**:79–85.
- Bethlehem RA, van Honk J, Auyeung B, and Baron-Cohen S (2013) Oxytocin, brain physiology, and functional connectivity: a review of intranasal oxytocin fMRI studies. *Psychoneuroendocrinology* **38**:962–974.
- Blatz AL and Magleby KL (1986) Single apamin-blocked Ca-activated K<sup>+</sup> channels of small conductance in cultured rat skeletal muscle. *Nature* **323**:718–720.
- Bonacci TM, Mathews JL, Yuan C, Lehmann DM, Malik S, Wu D, Font JL, Bidlack JM, and Smreka AV (2006) Differential targeting of Gbetagamma-subunit signaling with small molecules. *Science* **312**:443–446.
- Boratyn GM, Schäffer AA, Agarwala R, Altschul SF, Lipman DJ, and Madden TL (2012) Domain enhanced lookup time accelerated BLAST. *Biol Direct* **7**:12.
- Born J, Lange T, Kern W, McGregor GP, Bickel U, and Fehm HL (2002) Sniffing neuropeptides: a transnasal approach to the human brain. *Nat Neurosci* **5**:514–516.
- Brambilla M, Cotelli M, Manenti R, Dagani J, Sisti D, Rocchi M, Balestrieri M, Pini S, Raimondi S, Savioiti FM, et al. (2016) Oxytocin to modulate emotional processing in schizophrenia: a randomized, double-blind, cross-over clinical trial. *Eur Neuropsychopharmacol* **26**:1619–1628.
- Busnelli M, Kleinau G, Muttenthaler M, Stoev S, Manning M, Bibic L, Howell LA, McCormick PJ, Di Lascio S, Braida D, et al. (2016) Design and characterization of superpotent bivalent ligands targeting oxytocin receptor dimers via a channel-like structure. *J Med Chem* **59**:7152–7166.
- Busnelli M, Saulière A, Manning M, Bouvier M, Galés C, and Chini B (2012) Functional selective oxytocin-derived agonists discriminate between individual G protein family subtypes. *J Biol Chem* **287**:3617–3629.
- Cavanaugh J, Carp SB, Rock CM, and French JA (2016) Oxytocin modulates behavioral and physiological responses to a stressor in marmoset monkeys. *Psychoneuroendocrinology* **66**:22–30.
- Che T, Sun H, Li J, Yu X, Zhu D, Xue B, Liu K, Zhang M, Kunze W, and Liu C (2012) Oxytocin hyperpolarizes cultured duodenum myenteric intrinsic primary afferent neurons by opening BK(Ca) channels through IP<sub>3</sub> pathway. *J Neurochem* **121**:516–525.
- Chini B, Mouillac B, Ala Y, Balestre MN, Trumpp-Kallmeyer S, Hoflack J, Elands J, Hibert M, Manning M, Jard S, et al. (1995) Tyr115 is the key residue for determining agonist selectivity in the V1a vasopressin receptor. *EMBO J* **14**:2176–2182.
- Chini B, Mouillac B, Balestre MN, Trumpp-Kallmeyer S, Hoflack J, Hibert M, Andriolo M, Pupier S, Jard S, and Barberis C (1996) Two aromatic residues regulate the response of the human oxytocin receptor to the partial agonist arginine vasopressin. *FEBS Lett* **397**:201–206.
- Christophersen P and Wulff H (2015) Pharmacological gating modulation of small- and intermediate-conductance Ca(2+)-activated K(+) channels (KCa2.x and KCa3.1). *Channels (Austin)* **9**:336–343.
- Crespi BJ (2016) Oxytocin, testosterone, and human social cognition. *Biol Rev Camb Philos Soc* **91**:390–408.
- Dravid SM and Murray TF (2004) Spontaneous synchronized calcium oscillations in neocortical neurons in the presence of physiological [Mg(2+)]<sub>i</sub>: involvement of AMPA/kainate and metabotropic glutamate receptors. *Brain Res* **1006**:8–17.

- Edwards G, Niederste-Hollenberg A, Schneider J, Noack T, and Weston AH (1994) Ion channel modulation by NS 1619, the putative BKCa channel opener, in vascular smooth muscle. *Br J Pharmacol* **113**:1538–1547.
- French JA, Taylor JH, Mustoe AC, and Cavanaugh J (2016) Neuropeptide diversity and the regulation of social behavior in New World primates. *Front Neuroendocrinol* **42**:18–39.
- Frijling JL (2017) Preventing PTSD with oxytocin: effects of oxytocin administration on fear neurocircuitry and PTSD symptom development in recently trauma-exposed individuals. *Eur J Psychotraumatol* **8**:1302652.
- Geisler I and Chmielewski J (2009) Cationic amphiphilic polyproline helices: side-chain variations and cell-specific internalization. *Chem Biol Drug Des* **73**:39–45.
- Gimpl G and Fahrenholz F (2001) The oxytocin receptor system: structure, function, and regulation. *Physiol Rev* **81**:629–683.
- Gravati M, Busnelli M, Bulgheroni E, Reversi A, Spaiardi P, Parenti M, Toselli M, and Chini B (2010) Dual modulation of inward rectifier potassium currents in olfactory neuronal cells by promiscuous G protein coupling of the oxytocin receptor. *J Neurochem* **114**:1424–1435.
- Guastella AJ and Hickie IB (2016) Oxytocin treatment, circuitry, and autism: a critical review of the literature placing oxytocin into the autism context. *Biol Psychiatry* **79**:234–242.
- Insel T, Cuthbert B, Garvey M, Heinssen R, Pine DS, Quinn K, Sanislow C, and Wang P (2010) Research domain criteria (RDoC): toward a new classification framework for research on mental disorders. *Am J Psychiatry* **167**:748–751.
- Ishii TM, Silvia C, Hirschberg B, Bond CT, Adelman JP, and Maylie J (1997) A human intermediate conductance calcium-activated potassium channel. *Proc Natl Acad Sci USA* **94**:11651–11656.
- Johnson ZV and Young LJ (2015) Neurobiological mechanisms of social attachment and pair bonding. *Curr Opin Behav Sci* **3**:33–44.
- Kirui JK, Xie Y, Wolff DW, Jiang H, Abel PW, and Tu Y (2010) Gbetagamma signaling promotes breast cancer cell migration and invasion. *J Pharmacol Exp Ther* **333**:393–403.
- Kosfeld M, Heinrichs M, Zak PJ, Fischbacher U, and Fehr E (2005) Oxytocin increases trust in humans. *Nature* **435**:673–676.
- Lamy C, Goodchild SJ, Weatherall KL, Jane DE, Liégeois JF, Seutin V, and Marrion NV (2010) Allosteric block of KCa2 channels by apamin. *J Biol Chem* **285**:27067–27077.
- Lee AG, Cool DR, Grunwald WC Jr, Neal DE, Buckmaster CL, Cheng MY, Hyde SA, Lyons DM, and Parker KJ (2011) A novel form of oxytocin in New World monkeys. *Biol Lett* **7**:584–587.
- Lee K, Rowe IC, and Ashford ML (1995) NS 1619 activates BKCa channel activity in rat cortical neurones. *Eur J Pharmacol* **280**:215–219.
- Light KC, Smith TE, Johns JM, Brownley KA, Hofheimer JA, and Amico JA (2000) Oxytocin responsivity in mothers of infants: a preliminary study of relationships with blood pressure during laboratory stress and normal ambulatory activity. *Health Psychol* **19**:560–567.
- Lin Y and Smrcka AV (2011) Understanding molecular recognition by G protein  $\beta\gamma$  subunits on the path to pharmacological targeting. *Mol Pharmacol* **80**:551–557.
- Ludwig M and Leng G (2006) Dendritic peptide release and peptide-dependent behaviours. *Nat Rev Neurosci* **7**:126–136.
- MacKinnon R and Miller C (1988) Mechanism of charybdotoxin block of the high-conductance, Ca<sup>2+</sup>-activated K<sup>+</sup> channel. *J Gen Physiol* **91**:335–349.
- Manning M, Stoev S, Chini B, Durrux T, Mouillac B, and Guillon G (2008) Peptide and non-peptide agonists and antagonists for the vasopressin and oxytocin V1a, V1b, V2 and OT receptors: research tools and potential therapeutic agents. *Prog Brain Res* **170**:473–512.
- Missig G, Ayers LW, Schulkun J, and Rosen JB (2010) Oxytocin reduces background anxiety in a fear-potentiated startle paradigm. *Neuropsychopharmacology* **35**:2607–2616.
- Murray TF and Siebenaller JF (1993) Differential susceptibility of guanine nucleotide-binding proteins to pertussis toxin-catalyzed ADP-ribosylation in brain membranes of two congeneric marine fishes. *Bio Bull* **185**:346–354.
- Murthy KS and Makhlof GM (1996) Opioid mu, delta, and kappa receptor-induced activation of phospholipase C-beta 3 and inhibition of adenylyl cyclase is mediated by Gi2 and G(o) in smooth muscle. *Mol Pharmacol* **50**:870–877.
- Nguyen HM, Singh V, Pressly B, Jenkins DP, Wulff H, and Yarov-Yarovsky V (2017) Structural insights into the atomistic mechanisms of action of small molecule inhibitors targeting the KCa3.1 channel pore. *Mol Pharmacol* **91**:392–402.
- Parker KJ, Oztan O, Libove RA, Sumiyoshi RD, Jackson LP, Karhson DS, Summers JE, Hinman KE, Motonaga KS, Phillips JM, et al. (2017) Intranasal oxytocin treatment for social deficits and biomarkers of response in children with autism. *Proc Natl Acad Sci USA* **114**:8119–8124.
- Parreiras-e-Silva LT, Vargas-Pinilla P, Duarte DA, Longo D, Espinoza Pardo GV, Dulor Finkler A, Paixão-Côrtes VR, Paré P, Rovaris DL, Oliveira EB, et al. (2017) Functional New World monkey oxytocin forms elicit an altered signaling profile and promotes parental care in rats. *Proc Natl Acad Sci USA* **114**:9044–9049.
- Pedersen CA, Gibson CM, Rau SW, Salimi K, Smedley KL, Casey RL, Leserman J, Jarskog LF, and Penn DL (2011) Intranasal oxytocin reduces psychotic symptoms and improves theory of mind and social perception in schizophrenia. *Schizophr Res* **132**:50–53.
- Petit-Jacques J, Sui JL, and Logothetis DE (1999) Synergistic activation of G protein-gated inwardly rectifying potassium channels by the betagamma subunits of G proteins and Na(+) and Mg(2+) ions. *J Gen Physiol* **114**:673–684.
- Phaneuf S, Europe-Finner GN, Varney M, MacKenzie IZ, Watson SP, and López Bernal A (1993) Oxytocin-stimulated phosphoinositide hydrolysis in human myometrial cells: involvement of pertussis toxin-sensitive and -insensitive G-proteins. *J Endocrinol* **136**:497–509.
- Qiu S, Yi H, Liu H, Cao Z, Wu Y, and Li W (2009) Molecular information of charybdotoxin blockade in the large conductance calcium-activated potassium channel. *J Chem Inf Model* **49**:1831–1838.
- Quynh Doan NT and Christensen SB (2015) Thapsigargin, origin, chemistry, structure-activity relationships and prodrug development. *Curr Pharm Des* **21**:5501–5517.
- Rankovic Z, Brust TF, and Bohn LM (2016) Biased agonism: an emerging paradigm in GPCR drug discovery. *Bioorg Med Chem Lett* **26**:241–250.
- Ren D, Lu G, Moriyama H, Mustoe AC, Harrison EB, and French JA (2015) Genetic diversity in oxytocin ligands and receptors in New World monkeys. *PLoS One* **10**:e0125775.
- Reversi A, Cassoni P, and Chini B (2005) Oxytocin receptor signaling in myoepithelial and cancer cells. *J Mammary Gland Biol Neoplasia* **10**:221–229.
- Rifkin RA, Moss SJ, and Slesinger PA (2017) G protein-gated potassium channels: a link to drug addiction. *Trends Pharmacol Sci* **38**:378–392.
- Ritter SL and Hall RA (2009) Fine-tuning of GPCR activity by receptor-interacting proteins. *Nat Rev Mol Cell Biol* **10**:819–830.
- Sack M, Spieler D, Witzelmann L, Epple G, Stich J, Zaba M, and Schmidt U (2017) Intranasal oxytocin reduces provoked symptoms in female patients with post-traumatic stress disorder despite exerting sympathomimetic and positive chronotropic effects in a randomized controlled trial. *BMC Med* **15**:40.
- Sanchez M and McManus OB (1996) Paxilline inhibition of the alpha-subunit of the high-conductance calcium-activated potassium channel. *Neuropharmacology* **35**:963–968.
- Sankaranarayanan A, Raman G, Busch C, Schultz T, Zimin PI, Hoyer J, Köhler R, and Wulff H (2009) Naphtho[1,2-d]thiazol-2-ylamine (SKA-31), a novel activator of KCa2 and KCa3.1 potassium channels, potentiates the endothelium-derived hyperpolarizing factor response and lowers blood pressure. *Mol Pharmacol* **75**:281–295.
- Sehgal P, Szalai P, Olesen C, Praetorius HA, Nissen P, Christensen SB, Engedal N, and Möller JV (2017) Inhibition of the sarco/endoplasmic reticulum (ER) Ca<sup>2+</sup>-ATPase by thapsigargin analogs induces cell death via ER Ca<sup>2+</sup> depletion and the unfolded protein response. *J Biol Chem* **292**:19656–19673.
- Staal RGW, Khayrullina T, Zhang H, Davis S, Fallon SM, Cajina M, Nattini ME, Hu A, Zhou H, Poda SB, et al. (2017) Inhibition of the potassium channel KCa3.1 by senicapoc reverses tactile allodynia in rats with peripheral nerve injury. *Eur J Pharmacol* **795**:1–7.
- Stoop R (2014) Neuromodulation by oxytocin and vasopressin in the central nervous system as a basis for their rapid behavioral effects. *Curr Opin Neurobiol* **29**:187–193.
- Strayer DS, Hoek JB, Thomas AP, and White MK (1999) Cellular activation by Ca<sup>2+</sup> release from stores in the endoplasmic reticulum but not by increased free Ca<sup>2+</sup> in the cytosol. *Biochem J* **344**:39–46.
- Sun X, Hirano AA, Brecha NC, and Barnes S (2017) Calcium-activated BKCa channels govern dynamic membrane depolarizations of horizontal cells in rodent retina. *J Physiol* **595**:4449–4465.
- Vargas-Pinilla P, Paixão-Côrtes VR, Paré P, Tovo-Rodrigues L, Vieira CM, Xavier A, Comas D, Pissinatti A, Sinigaglia M, Rigo MM, et al. (2015) Evolutionary pattern in the OXT-OXTR system in primates: coevolution and positive selection footprints. *Proc Natl Acad Sci USA* **112**:88–93.
- Vergara C, Latorre R, Marrion NV, and Adelman JP (1998) Calcium-activated potassium channels. *Curr Opin Neurobiol* **8**:321–329.
- Wallis M (2012) Molecular evolution of the neurohypophysial hormone precursors in mammals: comparative genomics reveals novel mammalian oxytocin and vasopressin analogues. *Gen Comp Endocrinol* **179**:313–318.
- Wang YF and Hattori GI (2007) Interaction of extracellular signal-regulated protein kinase 1/2 with actin cytoskeleton in supraoptic oxytocin neurons and astrocytes: role in burst firing. *J Neurosci* **27**:13822–13834.
- Whiteaker KL, Gopalakrishnan SM, Groebe D, Shieh CC, Warrior U, Burns DJ, Coghlan MJ, Scott VE, and Gopalakrishnan M (2001) Validation of FLIPR membrane potential dye for high throughput screening of potassium channel modulators. *J Biomol Screen* **6**:305–312.
- Wulff H, Miller MJ, Hansel W, Grissmer S, Cahalan MD, and Chandy KG (2000) Design of a potent and selective inhibitor of the intermediate-conductance Ca<sup>2+</sup>-activated K<sup>+</sup> channel, IKCa1: a potential immunosuppressant. *Proc Natl Acad Sci USA* **97**:8151–8156.
- Young LJ and Barrett CE (2015) Neuroscience. Can oxytocin treat autism? *Science* **347**:825–826.
- Zhou XB, Lutz S, Steffens F, Korth M, and Wieland T (2007) Oxytocin receptors differentially signal via Gq and Gi proteins in pregnant and nonpregnant rat uterine myocytes: implications for myometrial contractility. *Mol Endocrinol* **21**:740–752.
- Zhou Y and Lingle CJ (2014) Paxilline inhibits BK channels by an almost exclusively closed-channel block mechanism. *J Gen Physiol* **144**:415–440.
- Zingg HH and Laporte SA (2003) The oxytocin receptor. *Trends Endocrinol Metab* **14**:222–227.

**Address correspondence to:** Thomas F. Murray, Department of Pharmacology, Creighton University School of Medicine, 2500 Omaha Plaza, Omaha, NE 68178. E-mail: tfmurray@creighton.edu